

Simulation of Dislocation Dynamics in Copper

Yoshiaki Kogure, Toshio Kosugi, Hirokazu Aoki, Tadatoshi Nozaki and Masao Doyama

Teikyo University of Science & Technology, Uenohara, Yamanashi 409-0193, Japan

Fax: 81-554-63-4431, e-mail: kogure@ntu.ac.jp

Atomistic configuration and motion of dislocation have been simulated by means of molecular dynamics method. The embedded atom method potential for copper is adopted in the simulation. Model crystal is a rectangular solid containing about 140,000 atoms. An edge dislocation is introduced along [112] direction near the centre of model crystal, and the system is relaxed. After the dislocation configuration is stabilized, a shear stress is applied and released. Wavy motion of dislocations is developed on the Peierls valleys when the free boundary condition is adopted. Propagation of phonon and dislocation-phonon interaction in the crystal are also simulated.

Key words: dislocation, molecular dynamics, embedded atom potential, copper, phonon

1. INTRODUCTION

The mechanical relaxation due to dislocation has been observed in copper, aluminum and other metals by means of internal friction measurements. Broad relaxation peaks observed at temperatures between 100 K and 200 K in the deformed samples are called Bordoni peak. If these relaxation peaks are analyzed based on the double kink formation mechanism, a larger value of Peierls stress, $10^{-3} \mu$, is derived, where μ is the shear modulus [1]. One of the present authors Kosugi discovered a new relaxation peak at 11 K in zone refined aluminum samples, and derived Peierls stress was orders of $10^{-5} \mu$, which is reasonable size as expected from the plastic deformation experiments [2]. Such a low temperature peak is not observed in impure samples and in other metals. On the other hand, we have performed a molecular dynamics computer simulation of dislocation motion in 2-dimensional model. In the simulation, the total kinetic energy is found to make a bump in the time variation, when the dislocation surmount a Peierls potential hill. The Peierls stress is estimated to be the order of $10^{-5} \mu$ from the size of the hump [3]. The purpose of the present study is to develop a 3-dimensional model for the simulation of dislocation in copper, and investigated the structure and motion of dislocations. A newly developed embedded atom method potential [4] was used in the present simulation. The potential function has successfully applied on the simulation of the dynamics of crystal defects and nanoparticles [5-7].

2. METHOD OF SIMULATION

Molecular dynamics simulation has been performed by using an EAM potentials. The potential functions are developed by the present authors [4]. The potential energy for i -th atom is expressed as

$$E_i = F(\rho_i) + (1/2) \sum \phi(r_{ij}) \quad (1)$$

where $F(\rho_i)$ is the embedding energy for i -th atom and ρ_i is the electron density function, which is a sum of the electron density of neighbor atoms labeled by j . These are expressed as

$$F(\rho_i) = D \rho_i \ln \rho_i, \quad (2-a)$$

$$\rho_i = \sum f(r_{ij}), \quad (2-b)$$

and $\phi(r_{ij})$ is the two body interaction between atom i and j . The functional form of $\phi(r_{ij})$ and $f(r_{ij})$ are

$$\phi(r_{ij}) = A(r_{c1} - r)^2 \exp(-c_1 r) \quad (3)$$

$$f(r_{ij}) = B(r_{c2} - r)^2 \exp(-c_2 r) \quad (4)$$

where $r_{c1} = 1.6 r_0$ and $r_{c2} = 1.9 r_0$ are the truncation distance of the potential, and r_0 is the nearest neighbor distance. The potential parameters for Cu are determined to reproduce the material properties such as the cohesive energy, the elastic constants, and the vacancy formation energy [4].

The time interval Δt for the simulation is chosen to be 1×10^{-15} s, which is less than 1/100 of the period of maximum atomic vibration frequency. Model crystal is surrounded by {110}, {111}, {112} faces, and consisted of 143,000 atoms. Sizes are about $12 \times 10 \times 10$ nm in x, y, z directions, respectively. Fixed or free boundary conditions are adopted, namely, atoms on the surfaces perpendicular to the dislocation line are fixed or released free. The dislocation is pinned down at the surfaces in the former. On the contrary the dislocation can move freely in the latter. Atoms on the surfaces parallel to the dislocation line are fixed in both cases during simulation. Initially a couple of extra {110} atomic planes are inserted in the lower middle of the crystal to introduce a dislocation, and the crystal is relaxed.

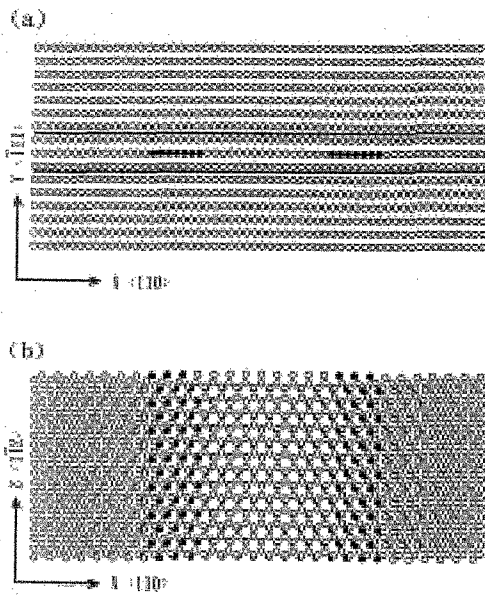


Fig. 1 Configuration of atoms around the split edge dislocation after the initial relaxation. (a) perpendicular, and (b) parallel to the dislocation lines.

The introduced dislocation is split to two partials as expected. One of the convenient way to express the position and the structure of dislocation is investigated by highlighting the atoms, which have larger potential energy than a certain criterion.

3. RESULTS AND DISCUSSION

3.1 Configuration after initial relaxation

Configuration of atoms after initial relaxation is shown in Fig. 1. The potential energy of each atom is calculated by equation (1), and the atoms with potential energy larger than -3.2 eV are represented by solid circles. The solid circles are concentrated at the dislocation cores, and introduced dislocation is seen to be split to partial dislocations. Vertical view of atomic planes surrounded by two straight lines in Fig.1(a) are shown in figure (b). A stacking fault structure is seen between two partial dislocations. Width of stacking fault is known to be determined as a balance of the stacking fault energy and the repulsive force between two partial dislocations, but the effect of fixed boundary may reduce the width of the stacking fault.

3.2 Motion of split dislocations

A shear strain $\varepsilon_{xy} = 0.05$ to move the dislocations in $-x$ direction was applied, and system was relaxed. Then the motion of dislocation was monitored. The simulation was performed at the temperature, 0 K, but it was slightly increased up to 5 K with the molecular dynamics (MD) time steps. Snap shots of the dislocation configuration at typical MD time steps are shown in Fig. 2 and Fig. 3, where only atoms with higher potential energy, $E > -3.5$ eV, are shown, and the atoms with the potential energy higher than -3.485 eV are shown

by solid circles. These open and solid circles characterize the internal structure of the dislocations. The dislocations are pinned at top and bottom surfaces by adopting the fixed boundary condition. Initially one of the partial dislocation move to right direction ($S=2000$), then another one follows. Both dislocations form bow shape as a balance of external stress and line tension of dislocations. On the contrary the dislocation shown in Fig. 3 are not fixed at the top and bottom surfaces, and they are free to move in x direction. The shape of dislocations are very wavy and many kinks seem to be present on the Peierls hills, which run in vertical direction on a slip plane. The configurations shown in Fig. 3 are not symmetrical in z direction. It is noted that six distinct types of atomic planes are stacked upon one another in a repeating sequence as ABCDEFABCDEF..... in $[112]$ direction, and it is not symmetric in a top and bottom direction. Initially the partial dislocation of left move towards left by the applied stress, afterwards it was pushed back by the mirror force due to the fixed boundary. These motions are repeated. A period of the dislocation oscillation is about 100 times of the period of thermal lattice vibration. As the dislocations are widely spread on a $\{111\}$ plane, they are always confined in a atomic plane, namely, the climb motion is not observed in the simulation.

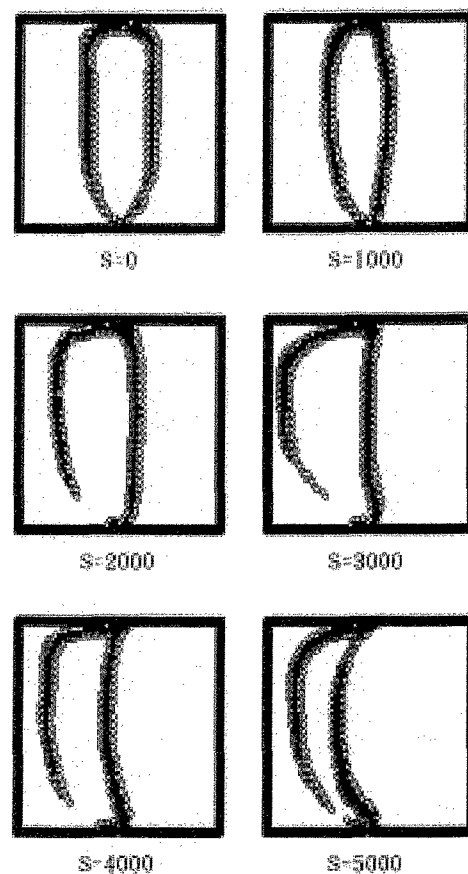


Fig. 2. Motion of a split edge dislocation under a fixed boundary condition. S shows the MD time steps.

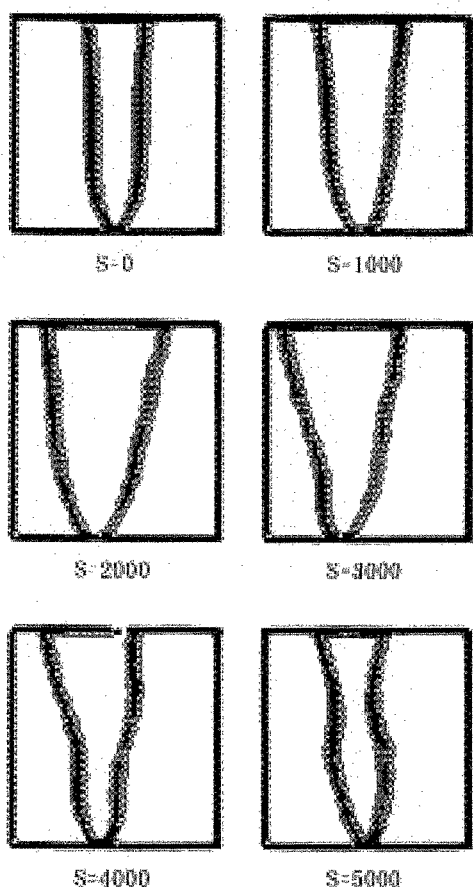


Fig. 3. Motion of a split edge dislocation under a free boundary condition. S shows MD time steps.

3.3 Change of potential energy

To investigate the relation between the motion of dislocation and potential energy of individual atom, mean potential energy E_{mean} was calculated for sampled atoms between two straight lines in Fig. 4. An example of the time variation of E_{mean} is shown in Fig. 5 (a). A sinusoidal oscillation of the energy is seen. Fig. 5 (b) shows the spatial distribution of the potential energy for sampled atoms at typical MD time steps marked by symbols A, B, C, D in Fig.5 (a). In the Fig.5 (b) background levels of the energy are arbitrarily shifted to separate the data points for different time steps. Two peaks in the spatial distribution of atomistic potential energy correspond to two partial dislocations. Excessive potential energy associated with a partial dislocation is about 0.5 eV, that is similar size with the elastically calculated dislocation self energy, $\mu b^3 / 4\pi$. It can be seen that a partial dislocation moves about unit length (Burgers vector b) of the crystal periodicity for a time, in which E_{mean} passes two minima of the potential energy. Then the oscillatory behavior seen in Fig. 5(a) is considered due to the effect of Peierls potential for the motion of partial dislocations. It is also noted that the

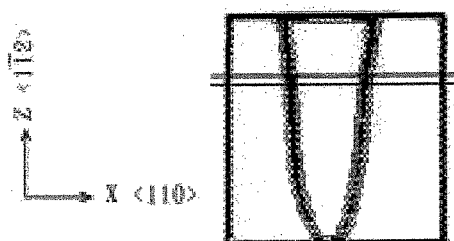


Fig. 4. Sampling of atoms for calculating mean potential energy E_{mean} . Atoms in an atomic row between two straight lines are sampled for calculation.

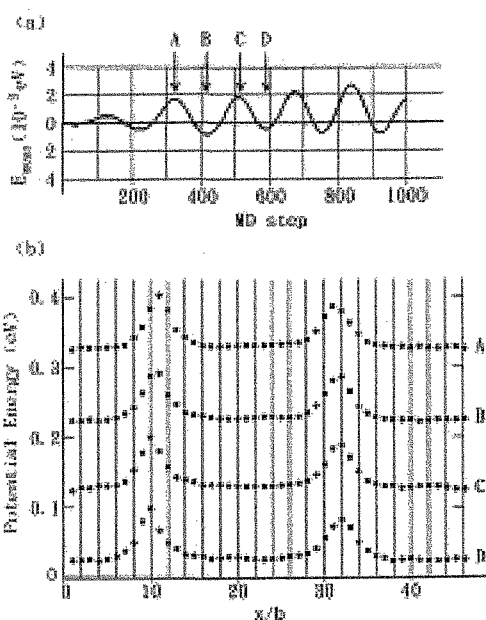


Fig. 5. Time variation of mean potential energy of atoms on the slip plane (a), and spatial variation of atomic potential energy at typical time steps, A, B, C, D. The peak correspond to the positions of split dislocations.

period of the vibration of E_{mean} is about 2×10^{-13} s, which is close to the period of lattice vibration the period of lattice vibration. This may suggest a phonon mediated motion of dislocations. A detailed analyses may reveal the dislocation motion by kink pair formation mechanism from atomistic point of view by molecular dynamics simulation.

3.4 Dislocation phonon interaction

An initial velocity in y-direction is given to the atoms near the centre of split partial dislocations, and the magnitude of the velocity of all atoms is monitored. Here, 'hot atom' is defined as an atom, which has larger vibration energy than environmental atoms. The simulations were performed in two samples of same size.

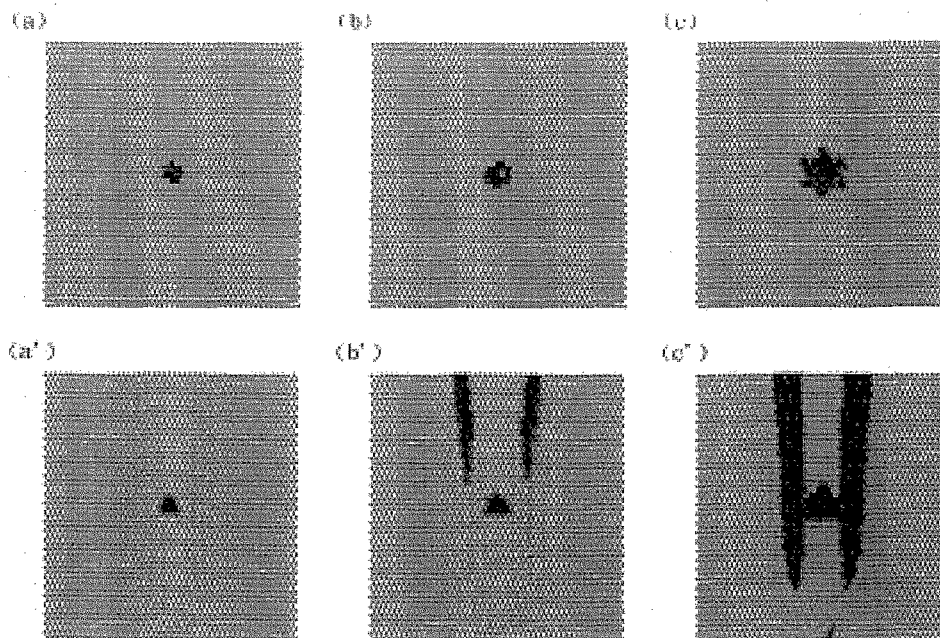


Fig. 6. Evolution of hot atoms (a) 100 MD steps, (b) 150 MD steps, (c) 200 MD steps in perfect crystal. Solid circles show 'hot atoms'. (a'), (b') and (c') show the results at same MD steps in crystals with dislocations.

One was the perfect crystal and the other contained split partials. Distribution of hot atoms at typical time step in both samples are compared in Fig. 6, in which the hot atoms are shown by solid circles. Initially hot atoms are generated between two partials. A region occupied by the hot atoms is growing. When the border of hot atoms reaches the position of the partial dislocations, many atoms constituting the dislocations are exited and become hot atoms. Atoms on the dislocation line are unstable and mobile, and they start to move by the excitations. The phenomenon may be described as the absorption of phonons by some localized dislocation modes, but quantitative discussion on the dislocation localized mode has not yet made. The molecular dynamics will provide a useful information on the problem.

4. CONCLUSION

EAM potential has successfully been applied on the molecular dynamics simulation of moving dislocations in a copper crystal. A dislocation was split to partials and a stacking fault appeared between partials. Motion of split partial dislocations are displayed by highlighting the atoms with larger potential energy. Wavy motion of

partial dislocations on a $\{111\}$ plane was observed under the free boundary condition. The time variation of the mean potential energy for atoms consisting dislocation was calculated and oscillation of the energy was observed. Propagation of phonons was also simulated and interaction with the atoms consisting dislocation core is observed.

REFERENCES

- [1] D.H.Niblet, in *Physical Acoustics*, Vol. IIIA, edited by W.P.Mason (Academic Press, Newyork, 1966) p.77.
- [2] T. Kosugi and T. Kino, *J. Phys. Soc. Jpn.* **58**,4269 (1989)
- [3] Y. Kogure and T. Kosugi, *J. Phys. IV (france)* Vol. **6**, pp. C8-195-198 (1996)
- [4] M. Doyama and Y. Kogure, *Radiat. Effects Defects Solids*, **142**, 107-114 (1997)
- [5] Y. Kogure, *J. Alloys Comp.*, **355**,188-195 (220)
- [6] Y. Kogure, T. Kosugi and M. Doyama, *Mater. Sci. Eng.* **A370**, 100-104 (2004)
- [7] Y. Kogure, T. Kosugi, M. Doyama and H. Kaburaki, *Mater. Sci. Eng.* **A442**, 71-74 (2006)

(Received December 26, 2007 ; Accepted December 29, 2007)